Journal of proteome research

Article

pubs.acs.org/jpr

Top-Down Proteomics of a Drop of Blood for Diabetes Monitoring

Pan Mao and Daojing Wang*

Newomics Inc., 5980 Horton Street, Suite 525, Emeryville, California 94608, United States

Supporting Information

ABSTRACT: The most common markers for monitoring patients with diabetes are glucose and HbA1c, but additional markers such as glycated human serum albumin (HSA) have been identified that could address the glycation gap and bridge the time scales of glycemia between transient and 2−3 months. However, there is currently no technical platform that could measure these markers concurrently in a cost-effective manner. We have developed a new assay that is able to measure glucose, HbA1c, glycated HSA, and glycated apolipoprotein A-I (apoA-I) for monitoring of individual blood glycemia, as well as cysteinylated HSA, S-nitrosylated HbA, and methionine-oxidized apoA-I for gauging oxidative stress and cardiovascular risks, all in 5 μL of blood. The assay utilizes our proprietary multinozzle emitter array chip technology to enable the analysis of small volumes of blood, without complex sample preparation prior to the online and on-chip liquid chromatography−nanoelectrospray ionization mass spectrometry. Importantly, the assay employs top-down proteomics for more accurate quantitation of protein levels and for identification of post-translational modifications. Further, the assay provides multimarker, multitime-scale, and multicompartment monitoring of blood glycemia. Our assay readily segregates healthy controls from Type 2 diabetes patients and may have the potential to enable better long-term monitoring and disease management of diabetes.

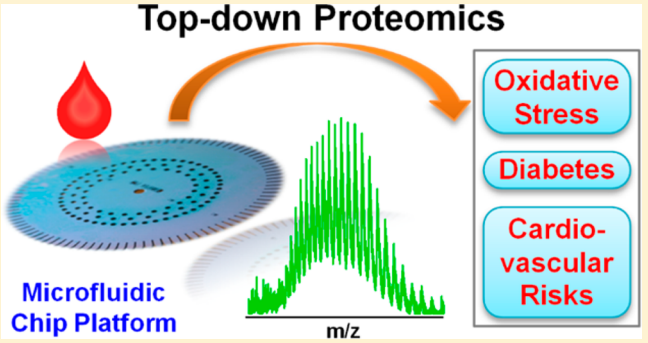

KEYWORDS: *MEA, microfluidic chip, top-down proteomics, LC−MS, blood, diabetes, multimarker*

INTRODUCTION

Diabetes has become a global epidemic, and its patient population will increase drastically in the coming years, according to the International Diabetes Federation. Despite its clinical diagnosis using fasting plasma glucose (FPG) and glycated hemoglobin A (HbA1c) assays[1] and home monitoring using blood glucose meters, one of the major challenges in diabetes management is the longitudinal monitoring of its progression and therapeutic responses. Glucose meters measure the transient blood glucose levels in the plasma, while HbA1c assays measure the average level of HbA glycation inside the red blood cells for the preceding 2−3 months.[2,3] The glycation gap, defined as the difference between the measured HbA1c and the HbA1c value predicted from glycated serum proteins, has been associated with microvascular complications of diabetes.[4,5] Therefore, efforts are ongoing to incorporate glycated albumin (GA) in the plasma, i.e., glycated human serum albumin (HSA), as an additional clinical marker for the average blood glucose level over a period of 2−3 weeks.[6] On the other hand, a variety of platforms and sample preparation protocols are utilized to measure glucose, HbA1c, and GA, separately, each using different methods based on liquid chromatography, immunoassay, electrochemistry, electrophoresis, etc.[2,3] Consequently, it is so far not a routine practice to perform parallel analysis of these markers under the same clinical settings and integrate the results in a timely manner. A unified platform that could concurrently measure multiple classes of diabetes markers, including but not limited to glucose, HbA1c, and GA, and encompass multiple time scales (e.g., transient, days, weeks, and months) of individual glycemia would make major contributions to diabetes theranostics and management.

Because the proteome reflects an individual's physiopathological states at a given time, proteomics is a powerful tool for diagnosing disease and monitoring progression and therapeutic responses. The majority of current clinical protein assays rely on the enzyme-linked immunosorbent assay (ELISA), which has the advantage of high sensitivity and ease of operation. However, ELISA suffers several significant limitations: (a) multiplexing greater than approximately 10 antibodies is difficult due to the cross-reactivity of antibodies; (b) antibodies are not available for the vast majority of proteins, particularly for their modified isoforms; and (c) assay development is lengthy and expensive. In contrast, mass spectrometry (MS) allows rapid and multivariate analysis of complex patterns of biomarkers without having specific antibodies available.[7,8] However, the penetration of MS-based proteomics into the *in vitro* diagnostics market has remained low.[9] MS-based platform has to achieve the (1) sensitivity, (2) throughput, and (3) robustness, comparable to or even better than those of ELISA, in order to find wider clinical acceptance. The focus of clinical

Received: October 30, 2013
Published: February 17, 2014

dx.doi.org/10.1021/pr401074t | J. Proteome Res. 2014, 13, 1560−1569

proteomics has been on analyzing low-abundance proteins using bottom-up proteomics (i.e., analysis of proteolytic peptides),[10−12] which faces the challenge of the huge dynamic range in biological fluids such as blood and urine and the difficulty of identifying all protein isoforms (or proteoforms),[13] including splicing, modifications, cleavages, etc., and quantifying their stoichiometry. There have been recent advances in top-down proteomics, i.e., large-scale identification and characterization of full-length proteins,[14−18] but its clinical potentials remain largely unexplored.[19,20] Mass spectrometry is making inroads into clinical diagnostics, which creates opportunities for new and improved assays.

In this work, we describe a new nanoflow liquid chromatography−mass spectrometry (LC−MS) assay, enabled by our silicon-microfluidic-chip platform, the multinozzle emitter array chip (MEA chip),[21−23] for rapid and multidimensional monitoring of diabetes, through direct top-down proteomics analysis of submicroliter volumes of human blood samples.

MATERIALS AND METHODS

Design, Manufacturing, Assembly, and Quality Control of MEA Chips

The single-plex MEA chips were designed using the L-Edit software (v15, Tanner Research). The fabrication procedures were similar to what we have described in detail.[21−23] However, the new design contained a three-layer Si−Si−glass structure that monolithically integrated several functional modules on a single chip (Figure 1a). Specifically, the electrospray emitters were constructed between the two silicon layers, while all other functional components (including the LC and trap columns) were built between the glass and silicon layers. A through-hole in the middle silicon layer was produced to connect emitters with LC channels. The silicon layers offer the ease for fabricating complex structures, while the glass cover provides the imaging window for real-time monitoring of on-chip processes such as the bead packing. MEA chips were examined by light microscope and scanning electron microscope (SEM) to confirm integrity of each component. For this work, the LC column was designed to be 5 cm (length) × 100 μm (width) × 100 μm (depth), and the trap column was 1 cm (length) × 300 μm (width) × 120 μm (depth). The microfabricated emitter had nozzles with a cross-section of 25 μm × 25 μm and a protruding length of 120 μm. The extraction segment was designed for analyte enrichment but was not utilized in this work.

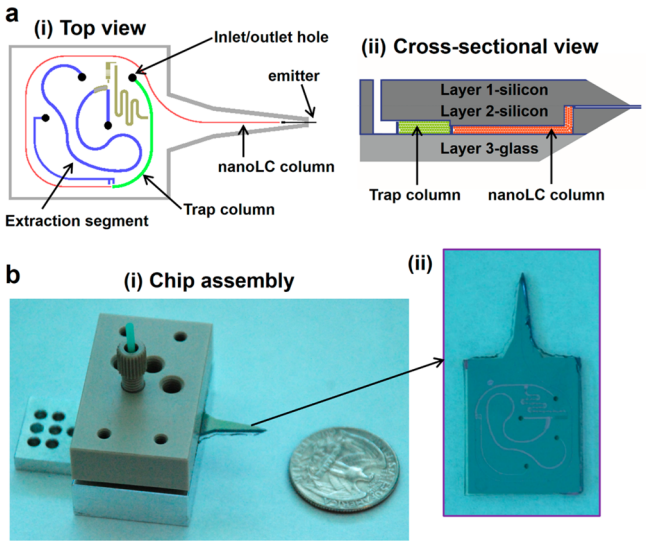

Figure 1. MEA chip for diabetes monitoring. (a) Schematics of the chip with the top-view (i) and cross-sectional view (ii). The chip contained a Si−Si−glass three-layer structure. The electrospray emitters were constructed between the two silicon layers. All other functional components including a trap column (green) and a LC column (red) were produced between the silicon and glass layers. The cross-sectional view is not to scale. (b) High-resolution photographs showing the chip and its assembly with a custom-built manifold and fittings, relative to a U.S. quarter. The dimensions of the LC column were 5 cm (length) × 100 μm (width) × 100 μm (depth), and the trap column was 1 cm (length) × 300 μm (width) × 120 μm (depth). The microfabricated emitter had nozzles with a cross-section of 25 μm × 25 μm and a protruding length of 120 μm.

To establish robust fluidic connections for high-pressure on-chip and online nanoLC separation, we built a manifold to mechanically assemble the MEA chip with capillary tubing connected to the outside nanoflow source (Figure 1b). The chip was sandwiched between a PEEK clamping plate and an aluminum plate and tightly clamped by screws with O-rings in-between to prevent the fluid leakage. The top PEEK plate had four threaded ports for Upchurch fittings to provide connections with capillary tubing. The assembly was then fastened to a translational stage, using a screw in the aluminum plate. High voltage was supplied to MEA chip via the conductive aluminum plate. No fluid leakage was observed for the MEA chip assembly for the flow under a pressure of over 2000 psi in our LC−MS runs.

For on-chip LC columns, a 3 μm frit was implemented between the LC channel and nozzles to retain beads. LC and trap channels were packed with Magic-C4 5 μm beads (pore size of 300 Å, Bruker-Michrom) using an in-house column packing station. Briefly, beads were suspended in methanol and sonicated to form a solution of monodispersed particles. Then the slurry of particles was forced into the channels on the chip through the sample input holes by a pressurized (>1000 psi) helium gas tank. The pressure gauge was shut off in 20 min, and the system was slowly depressurized for about 1 h before switching to the atmosphere pressure. Helium gas was purged afterward to dry out the bead beds. Finally, the backend of the packed channels were sealed by fabricating sol−gel frits[24] to prevent beads from retreating during the LC runs. The sol−gel solution was prepared by mixing 34 μL of Kasil 1 potassium silicate (PQ Corp.) with 6 μL of formamide (Sigma), followed by vortexing and centrifuging for 1 min. A 1 μL aliquot of the sol−gel solution was introduced to a chip reservoir and then flowed into the channel for 2 min.[24] The chip was then incubated on a hot plate at 80 °C for over 6 h. After the frit was completely polymerized, the columns with sol−gel frits were washed with methanol. The quality and reproducibility of frit fabrication and bead packing were confirmed by microscopic examination, followed by backpressure monitoring for the LC channels under a constant flow rate (e.g., 1 μL/min). The efficiency of the LC separation was validated by LC−MS analysis of standard proteins mixtures. Since our on-chip channels were built on inert silicon substrate, we followed the standard protocols for conventional cartridge columns to regenerate LC and trap channels.

dx.doi.org/10.1021/pr401074t | J. Proteome Res. 2014, 13, 1560−1569

Preparation of Standard Samples for Validating MEA Chips

Pure HbA1c and HbA0 (IFCC reference material) were obtained from Lee Biosolutions (St. Louis, MO). Lyphochek hemoglobin A1c linearity set (lot no. 34650, level 1−4) was obtained from Bio-Rad (Hercules, CA). All other chemicals and biologics were obtained from Sigma-Aldrich (St. Louis, MO). For ESI-MS response curve of HbA1c/HbA, calibrator solutions were prepared by mixing pure HbA0 and HbA1c solutions in LC solvent A (5/95 acetonitrile (ACN)/H_2O with 0.2% formic acid (FA)). A set of calibrators with five levels of HbA1c (0, 1.9%, 5.7%, 10.7%, and 16.7%) were prepared in triplicate, and each replicate was analyzed at least 3 times. HbA1c linearity set samples were stored at −20 °C. Right before use, they were thawed, incubated at 37 °C for 10 min, and then diluted 1:1000 in solvent A for LC−MS analysis. For LC−MS response curve of glucose/D-(+) glucose-6,6-d_2 (hereafter: glucose-d_2), calibrator solutions were prepared by mixing pure glucose and glucose-d_2 solutions and subequently spiked in the pooled plasma that was diluted 1:100 in solvent A. The concentration of glucose-d_2 in the final solution was fixed at 50 μM. A set of calibrators with five concentrations of glucose (0, 20, 50, 100, and 250 μM) were prepared in triplicate, and each replicate was analyzed at least 3 times.

Processing of Blood Samples for LC−MS Analysis

Fresh whole blood from both healthy control donors (n = 8) and type 2 diabetes (T2D) patients (n = 8) and frozen pooled plasma were obtained from Innovative Research Inc. (Novi, MI). The fresh blood samples were collected in the presence of EDTA and shipped on ice by FedEx to Newomics Inc. within 2−3 days after collection. Aliquots of whole blood samples were stored at 4 °C upon arrival and analyzed within 2−5 days of receipt in order to collect the data described in this work. A 5 μL aliquot of each whole blood sample was diluted with 10 μL of 1× PBS buffer, and afterward the mixture was centrifuged at a speed of 3,000g for 5 min at room temperature (RT). A 5 μL aliquot of the supernatant was reconstituted in 36.7 μL of LC solvent A and subsequently centrifuged at 14,000g for 5 min at RT to remove any cellular debris. A total of 35 μL of supernatant was collected and stored as the plasma portion, with a final concentration of 1:25 dilution of the beginning whole blood sample. The cell pellet derived from the first centrifuge step was washed with 1× PBS buffer at RT three times and then incubated with 50 μL of 1× PBS for 2 h at 37 °C to remove the labile pre-HbA1c (Schiff base, also called aldimine).[25] The cells were subsequently lyzed by suspending the cell pellet in 25 μL of HPLC-grade water and vortexing for 5 min at RT. The hemolysate was then constituted in 470 μL of LC solvent A and centrifuged at 14,000g for 5 min. A total of 450 μL of supernatant was collected and stored as the hemolysate portion, with a final concentration of 1:100 dilution of the beginning whole blood sample. Finally, an artificial mixture of a 40 μL solution was generated by mixing 10 μL of 200 μM glucose-d_2 standards, 10 μL of its plasma portion (1:25 dilution), 0.4 μL of its hemolysate portion (1:100 dilution), and 19.6 μL of LC solvent A. A 4 μL aliquot of the mixture, representing 0.1 μL of each whole blood sample, was injected for LC−MS analysis to generate the data shown in Figure 2. Samples were prepared in triplicate, and each replicate was analyzed at least 3 times.

LC−MS Analysis Using MEA Chips

A capillary liquid chromatography system (CapLC) (Waters Corp.) was used to deliver nanoflow LC gradient on the MEA chip. A volume of 4 μL of the processed mixture (see above) was injected through an autosampler into the on-chip trap column with a flow rate of 20 μL/min. The on-chip LC column was run at a flow rate of 600 nL/min. The solvent A consisted of 5/95 ACN/H_2O with 0.2% FA, and solvent B consisted of 95/5 ACN/H_2O with 0.2% FA. The LC gradient started at 1% B and was hold at 1% B for 3 min. Starting at 3 min, it was linearly increased to 20% B in 5 min and then ramped up again to 50% in 42 min. After that, it was increased to 95% B in 5 min and finally returned to the initial condition (1% B) in another 5 min. MS detection was performed using a hybrid quadrupole/orthogonal Q-TOF API US mass spectrometer (Waters Corp.) with the same MS and MS/MS settings as we described before.[21−23] The capillary voltage was set to be 3.2 kV, and cone voltage was 40 V. Nanoelectrospray process on MEA emitters was visualized and monitored using a Waters nanoflow camera kit equipped with the MLH-10x Zoom lenses (Computar).

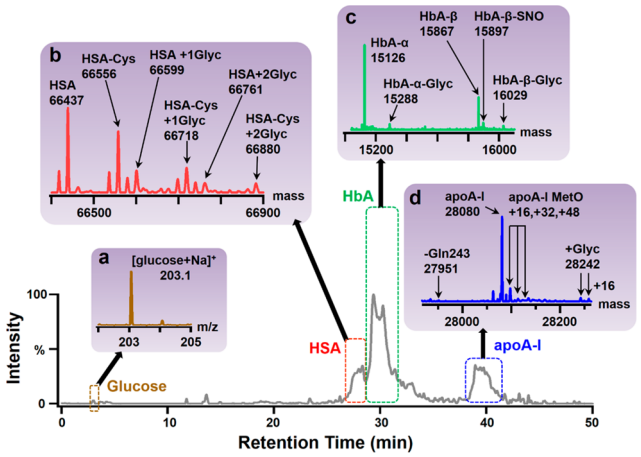

Figure 2. A top-down-proteomics-centric assay using small volumes of blood samples. Representative total ion chromatogram (TIC) for a 1-h LC−MS run of ∼0.1 μL whole blood, showing LC−MS peaks for free glucose, HSA, HbA, and apoA-I, respectively. The representative mass spectra of glucose and different isoforms of HSA, HbA, and apoA-I after MaxEnt 1 deconvolution are shown in inserts a−d, respectively. The identified protein modifications include glycation, cysteinylation, nitrosylation, oxidation, and truncation.

Data Analysis

The raw LC−MS data were processed using the MassLynx 4.0 software package provided with the Q-TOF instrument. Extracted ion chromatograms (EIC) for all target proteins were generated using their corresponding ions of the charge state at the maximum intensity. The entire peak region in the EIC for each protein was summed to acquire their integrated mass spectra. The integrated mass spectrum (m/z 750−1350 for HbA and apoA-I, m/z 1100−1400 for HSA) was then deconvoluted onto a mass scale using the maximum entropy-based algorithm (MaxEnt 1) in MassLynx 4.0. The parameters for MaxEnt 1 were chosen as the following: mass range 12,000−18,000 Da for HbA, 63,000−69,000 Da for HSA, and 24,000−32,000 Da for apoA-I; resolution 0.1−0.2 Da/channel. The uniform Gaussian peak width at the half-height for each protein was determined using its highest intensity peak. The left and right minimum intensity ratio was set to be 40% for HbA, 85% for HSA, and 80% for apoA-I. Finally, the MaxEnt 1 deconvoluted spectrum was baseline-subtracted with a 25-order polynomial, smoothed (2 × 6 Da Savitzky-Golay), and centered

dx.doi.org/10.1021/pr401074t | J. Proteome Res. 2014, 13, 1560−1569

(centroid top 80%) with areas created. The ion intensities in the centered spectra, which employed the corresponding peak areas, were used to quantify each protein isoform. For HbA1c, the MS response curve was generated using the pure protein standards. For HSA and apoA-I isoforms, we assumed similar MS responses for unmodified proteins and their different adducts (e.g., HSA-Cys and HSA-Glyc) in this work. Following are the details for calculating the relative level of each protein isoform.

HbA1c value was calculated using the ratio between the peak area (I) of the charge deconvoluted peak of HbA-β-Glyc (mass, 16029 Da) and those of all prominent HbA-β isoforms including HbA-β (mass, 15867 Da), HbA-β-SNO (mass, 15897 Da), and HbA-β-Glyc and normalized by the ESI-MS response factor determined from the slope of the response curve in Figure 3a. The equation is

$$\text{HbA1c} = I(\text{HbA-}\beta\text{-Glyc})/((I(\text{HbA-}\beta) + I(\text{HbA-}\beta\text{-SNO}) + I(\text{HbA-}\beta\text{-Glyc})) \times 0.9516)$$

, where I represents the peak area of the charge-deconvoluted peaks, and 0.9516 is the response factor.

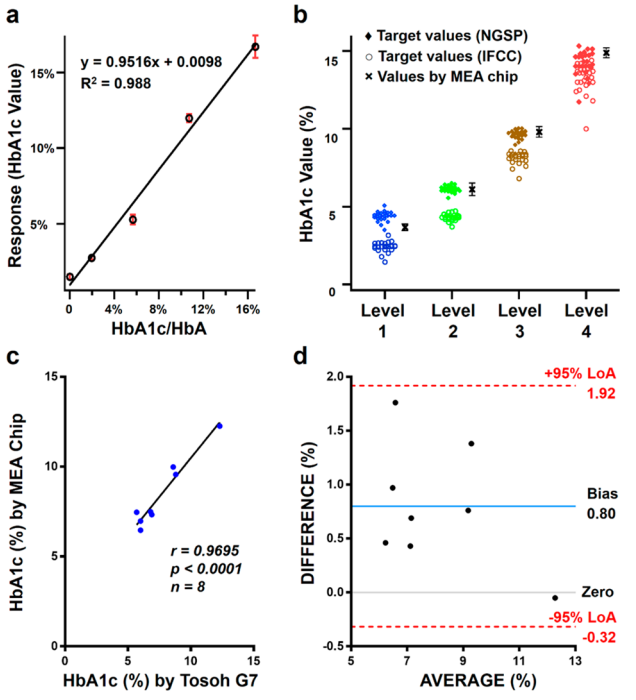

Figure 3. Validation of a top-down-proteomics-centric assay for diabetes monitoring. (a) Calibration curve for the ratio of HbA1c:HbA determined by our assay for known molar ratios of the mixtures of purified HbA1c and HbA0. (b) Comparison of HbA1c values for the Lyphochek Hemoglobin A1c linearity set samples (LOT 34650), obtained by our MEA chip-based assay (×), and the corresponding target values using other commercial assays (NGSP (♦) and IFCC (○)) provided by Bio-Rad. Error bars, SD ($n \geq 3$) for our assay. (c, d) Comparison of HbA1c values for blood samples from T2D patients (n = 8), each measured by our MEA chip and a commercial Tosoh G7 HPLC analyzer, respectively, showing the correlation between the values obtained by the two methods (Pearson's correlation, r = 0.9695, p < 0.0001, n = 8) (c) and the Bland-Altman plot of the difference between the two methods. The lines were plotted indicating the bias (0.80%) and the upper and lower limits of agreement (LoA) (bias ±2 × SD) (d).

Similarly, the relative level of HbA-SNO was calculated as

$$\text{HbA-SNO} = I(\text{HbA-}\beta\text{-SNO})/(I(\text{HbA-}\beta) + I(\text{HbA-}\beta\text{-SNO}) + I(\text{HbA-}\beta\text{-Glyc}))$$

The relative level of glycated albumin (GA) was calculated as

$$\text{GA} = (I(\text{HSA} + 1\text{Glyc}) + I(\text{HSA-Cys} + 1\text{Glyc}) + 2 \times I(\text{HSA} + 2\text{Glyc}) + 2 \times I(\text{HSA-Cys} + 2\text{Glyc}))/(I(\text{HSA}) + I(\text{HSA-Cys}) + I(\text{HSA} + 1\text{Glyc}) + I(\text{HSA-Cys} + 1\text{Glyc}) + I(\text{HSA} + 2\text{Glyc}) + I(\text{HSA-Cys} + 2\text{Glyc}))$$

We used the double weighting of the doubly glycated form of HSA to account for two glycations per HSA. The denominator contained all identifiable HSA peaks and represented the total HSA.

The relative level of HSA-Cys was calculated as

$$\text{HSA-Cys} = (I(\text{HSA-Cys}) + I(\text{HSA-Cys} + 1\text{Glyc}) + I(\text{HSA-Cys} + 2\text{Glyc}))/(I(\text{HSA}) + I(\text{HSA-Cys}) + I(\text{HSA} + 1\text{Glyc}) + I(\text{HSA-Cys} + 1\text{Glyc}) + I(\text{HSA} + 2\text{Glyc}) + I(\text{HSA-Cys} + 2\text{Glyc}))$$

The relative level of apoA-I glycation (GapoA-I) was calculated as

$$\text{GapoA-I} = (I(\text{apoA-I} + 1\text{Glyc}) + I(\text{apoA-I} + 1\text{Glyc} + 1\text{MetO}) + I(\text{apoA-I} + 1\text{Glyc} + 2\text{MetO}) + I(\text{apoA-I} + 1\text{Glyc} + 3\text{MetO}))/(I(\text{apoA-I} - \text{Gln}) + I(\text{apoA-I} - \text{Gln} + 1\text{MetO}) + I(\text{apoA-I} - \text{Gln} + 2\text{MetO}) + I(\text{apoA-I} - \text{Gln} + 3\text{MetO}) + I(\text{apoA-I}) + I(\text{apoA-I} + 1\text{MetO}) + I(\text{apoA-I} + 2\text{MetO}) + I(\text{apoA-I} + 3\text{MetO}) + I(\text{apoA-I} + 1\text{Glyc}) + I(\text{apoA-I} + 1\text{Glyc} + 1\text{MetO}) + I(\text{apoA-I} + 1\text{Glyc} + 2\text{MetO}) + I(\text{apoA-I} + 1\text{Glyc} + 3\text{MetO}))$$

The denominator contained all identifiable apoA-I peaks and represented the total apoA-I.

The relative level of methionine oxidation of apoA-I (apoA-I MetO) was calculated as the percentage of maximum methionine oxidation capacity of apoA-I, in which all apoA-I molecules are modified by 3 methionine sulfoxides.[26] The intensity of unoxidized, singly, doubly, and triply oxidized apoA-I were multiplied by 0, 1/3, 2/3, and 1, respectively, and then summed to obtain the weighted intensity of the oxidized apoA-I. We considered MetO of all apoA-I isoforms. Hence,

dx.doi.org/10.1021/pr401074t | J. Proteome Res. 2014, 13, 1560−1569

apoA-I MetO was obtained by normalizing the weighted intensity of oxidized apoA-I with that of the total apoA-I as

$$\begin{aligned}\text{apoA-I MetO} = {} & (I(\text{apoA-I} - \text{Gln} + 1\text{MetO}) \times \frac{1}{3} \\ & + I(\text{apoA-I} - \text{Gln} + 2\text{MetO}) \times \frac{2}{3} \\ & + I(\text{apoA-I} - \text{Gln} + 3\text{MetO}) \\ & + I(\text{apoA-I} + 1\text{MetO}) \times \frac{1}{3} \\ & + I(\text{apoA-I} + 2\text{MetO}) \times \frac{2}{3} \\ & + I(\text{apoA-I} + 3\text{MetO}) \\ & + I(\text{apoA-I} + 1\text{Glyc} + 1\text{MetO}) \times \frac{1}{3} \\ & + I(\text{apoA-I} + 1\text{Glyc} + 2\text{MetO}) \times \frac{2}{3} \\ & + I(\text{apoA-I} + 1\text{Glyc} + 3\text{MetO}) \\ & /(I(\text{apoA-I} - \text{Gln}) + I(\text{apoA-I} - \text{Gln} \\ & + 1\text{MetO}) + I(\text{apoA-I} - \text{Gln} + 2\text{MetO}) \\ & + I(\text{apoA-I} - \text{Gln} + 3\text{MetO}) \\ & + I(\text{apoA-I}) + I(\text{apoA-I} + 1\text{MetO}) \\ & + I(\text{apoA-I} + 2\text{MetO}) \\ & + I(\text{apoA-I} + 3\text{MetO}) \\ & + I(\text{apoA-I} + 1\text{Glyc}) \\ & + I(\text{apoA-I} + 1\text{Glyc} + 1\text{MetO}) \\ & + I(\text{apoA-I} + 1\text{Glyc} + 2\text{MetO}) \\ & + I(\text{apoA-I} + 1\text{Glyc} + 3\text{MetO})\end{aligned}$$

For statistical analyses, we utilized the GraphPad Prism 6 (GraphPad Software Inc., La Jolla, CA). For error bars at each data point, at least triplicate experiments ($n \geq 3$) were performed to obtain the standard deviation. A Bland-Altman plot was used for comparison between our assay using a MEA chip and the commercial HbA1c assay using a Tosoh G7 instrument. Student's t test was performed to examine the differences between controls and T2D patients for HbA1c, GA, GapoA-I, HSA-Cys, HbA-SNO, and apoA-I MetO, respectively. The p values of the t test were determined by using the unpaired and two-tailed parametric tests without assuming equal variance in both groups. Pearson's correlation was performed to investigate the following relationships: (1) between any two of HbA1c, GA, and GapoA-I; (2) between HSA-Cys and HbA1c, GA, and GapoA-I, respectively; and (3) between age and HSA-Cys, HbA-SNO, and apoA-I MetO, respectively. Pearson's coefficient (r) and p value (two-tailed) were calculated. A p value ≤ 0.05 was considered statistically significant.

RESULTS

We developed a MEA chip for top-down-proteomics-centric analysis of small volumes of blood samples. Figure 1b shows an assembly of our one-plex MEA chip (chip itself is shown in the insert) used for this study. We first demonstrated qualitative and quantitative LC−MS analyses of free glucose and abundant blood proteins relevant to hyperglycemia in diabetes including hemoglobin A (HbA), human serum albumin (HSA), and apolipoprotein A-I (apoA-I) (Figure 2). Using glucose-d_2 as the internal standard, we could accurately determine the free glucose concentrations in the blood using the ratio between the LC−MS peak areas of the Na+ adducts of glucose and glucose-d_2 (m/z 203 and 205, respectively) (Supplementary Figure 1). Because glucose has a low hydrophobicity, it was eluted very early in our current 1-h LC gradient on the C4 column that was optimized for LC−MS analysis of proteins. However, we were still able to obtain the response curve and quantify glucose from the LC−MS chromatograms. Since glucose degrades quickly in the whole blood and needs to be measured immediately after the blood draw, we did not quantify the glucose level in individual whole blood samples in this work. In the future, we could also analyze glucose in a separate column packed with HILIC (e.g., NH_2) beads on a 24-plex MEA chip if necessary. We next showed quantitation of various isoforms of HSA, HbA, and apoA-I in a pooled plasma sample or a fresh whole blood sample from a healthy individual. We first performed LC−MS analysis of standard protein mixtures to validate the performance of the on-chip C4 column on our MEA chip (Supplementary Figure 2). We then analyzed diluted blood samples corresponding to a mere 0.1 μL of the starting plasma using our MEA chip. By comparing the LC−MS chromatograms, MS spectra, charge states, and MaxEnt 1 transformed charge-deconvoluted peaks (inserts) (Figure 2), we identified various modifications (cysteinylation, glycation, nitroslylation, methionine oxidation, etc.) of these proteins in the blood, consistent with the earlier published works.[26−29] Specifically, for HSA, we detected its multiple species, including unmodified, cysteinylated (at Cys34), glycated (dominantly at Lys525), both cysteinylated and glycated, and doubly glycated isoforms; for HbA, we identified glycation at both α and β chains, and nitrosylation at β chain (at Cys93); for apoA-I, we identified glycation (hereafter: GapoA-I), oxidation at 1−3 methionine residues (hereafter: apoA-I MetO), etc. Protein nitrosylation and cysteinylation at cysteine residues are important for signal transduction in response to oxidative stress,[30] while glycation of HbA (and HSA) is a known marker for glucose metabolism and widely used for diabetes diagnosis.

We next developed and validated our assay for diabetes monitoring. Using HbA1c (HbA glycated at the N-terminus of β chain) as the example, we worked out the LC−MS calibration curve for the HbA1c/HbA ratio and obtained a response factor of 0.9516 (Figure 3a). Based on this response curve, we determined the HbA1c values for the Bio-Rad Lyphochek Hemoglobin A1c linearity set, which contains standard samples to check linearity and verify calibration of commercial instruments for HbA1c assays (Figure 3b). We plotted the target values of HbA1c for different platforms provided in the Bio-Rad technical datasheet along with the values determined by our MEA chip platform. As expected, the values for National Glycohemoglobin Standardization Program (NGSP)-based methods were grouped higher than those for International Federation of Clinical Chemistry and Laboratory Medicine (IFCC)-based methods (typically +1.5−2.0%)[2,3] [Note: IFCC % was used in the plot as provided in the datasheet; however, IFCC values are now generally reported in mmol/mol]. NGSP-based methods measure the percentage of HbA1c in total HbA at the protein level, while IFCC-based methods measure the ratio between glycated and nonglycated hexapeptides of HbA at

dx.doi.org/10.1021/pr401074t | J. Proteome Res. 2014, 13, 1560−1569

the peptide level after enzymatic digestions.[2,3,25] The values from our LC−MS assay were consistent with these target values. Therefore, our nanoflow LC−MS assay using a MEA chip is suitable for quantifying protein glycation as glycemia markers for diabetes. We further confirmed that the HbA1c values determined by our assay were consistent with those obtained using conventional methods. As shown in Figure 3c and d, our results for the 8 blood samples from T2D patients agreed very well with those obtained by the commercial Tosoh G7 HPLC platform (NGSP method) (Figure 3c: Pearson's correlation, $r = 0.9695$, $p < 0.0001$, two-tailed; and Figure 3d: Bland-Altman Plot, limit of agreement (LoA), $p < 0.0500$).

We then demonstrated proof-of-principle applications of our assay for monitoring individual glycemia. We analyzed fresh blood samples from a total of 16 individuals (8 healthy controls; 8 Type 2 diabetes, T2D). We compared the values of HbA1c, GA, and GapoA-I between controls and T2D (Figure 4a−c). The mean values were significantly higher in T2D than

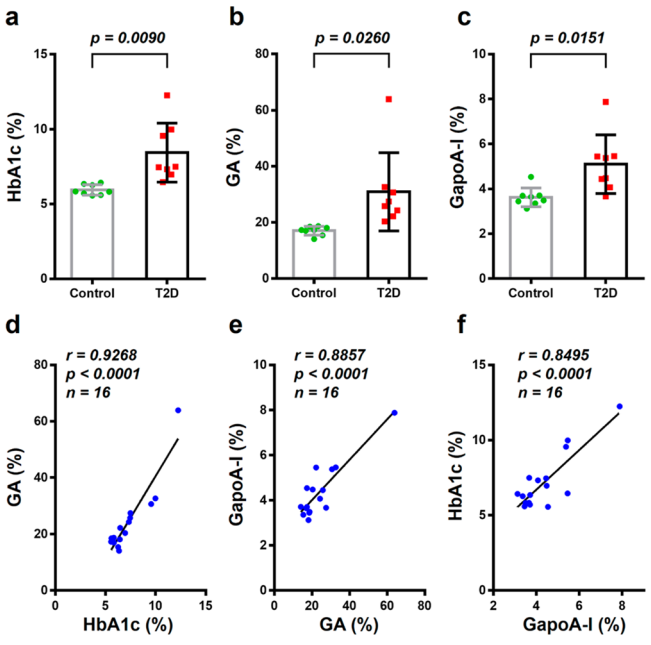

Figure 4. Application of the assay for monitoring individual glycemia. (a, b, c) Quantitation of the glycation levels of HbA (HbA1c), HSA (GA), and apoA-I (GapoA-I) in controls and Type 2 diabetes (T2D) patients, respectively ($n = 8$ for each group). The mean HbA1c, GA, and GapoA-I levels in T2D were 8.44%, 30.93%, and 5.10%, respectively, while in controls they were 5.95%, 17.05%, and 3.63%, respectively. The p values were calculated using the two-tailed Student's t test. (d, e, f) Correlation between any two values of HbA1c, GA, and GapoA-I, respectively, for each individual monitored in (a−c) (Pearson's correlation, $p < 0.0001$, $n = 16$).

in controls, with 8.44% and 5.95% for HbA1c, 30.93% and 17.05% for GA, and 5.10% and 3.63% for GapoA-I, respectively. Further, we could completely segregate controls from T2D using these markers (Student's t test, $p = 0.0090$, 0.0260, 0.0151 for HbA1c, GA, and GapoA-I, respectively). We next evaluated the relationship between each two of these three markers for the total 16 samples analyzed (Figure 4d−f). All correlated strongly to each other, with $r = 0.9268$, 0.8857, and 0.8495 (Pearson's correlation, $p < 0.0001$, two-tailed), between HbA1c and GA, GA and GapoA-I, and GapoA-I and HbA1c, respectively. On the basis of the average *in vivo* lifetime of their unmodified proteins, HbA1c, GA, GapoA-I could manifest the average blood glucose level over a period of 2−3 months, 2−3 weeks, and 1−2 days,[31] respectively. Therefore, the degree of mutual correlations matches the degree of difference in time scales that these markers represent.

Finally, we showed that our assay could provide additional information about oxidative stress and cardiovascular risks for individuals. There is a strong interplay between oxidative stress and diabetes, and the most severe consequences of diabetes are cardiovascular diseases including atherosclerosis.[32] As already shown in Figure 2, our LC−MS assay concurrently detected HSA-Cys, HbA-SNO, and apoA-I MetO, well-known protein markers for oxidative stress in plasma, hypoxic vasodilation, and oxidative status of high-density lipoprotein (HDL), respectively.[30,33−35] We compared the values of these markers for controls and T2D (Figure 5a−c). We observed a significant

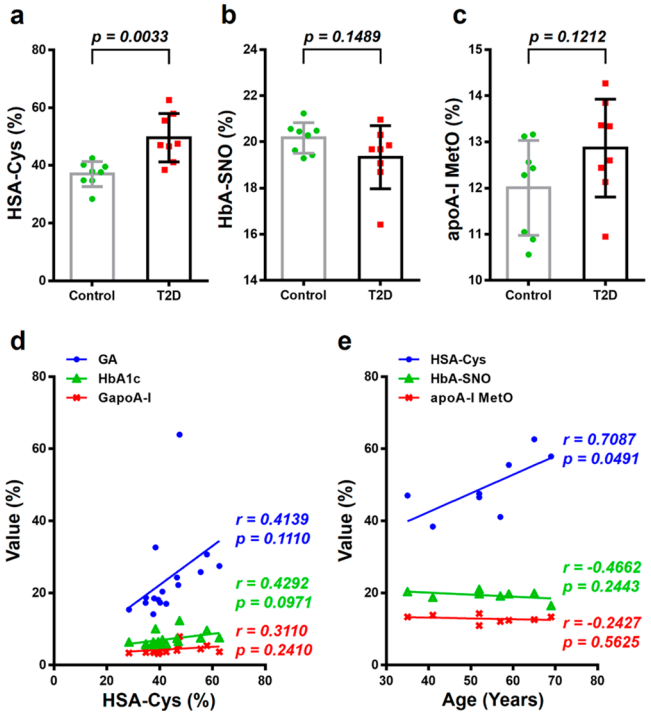

Figure 5. Application of the assay for concurrently monitoring individual oxidative stress and cardiovascular risks. (a, b, c) Comparison of the levels of HSA cysteinylation (HSA-Cys), hemoglobin S-nitrosylation (HbA-SNO), and apoA-I oxidation (apoA-I MetO), between controls and T2D patients, respectively ($n = 8$ for each group). The mean HSA-Cys, HbA-SNO, and apoA-I MetO levels in T2D were 49.59%, 19.33%, and 12.87%, respectively, while in controls they were 36.96%, 20.17%, and 12.01%, respectively. The p values were calculated using the two-tailed Student's t test. (d) Correlation between the levels of HSA-Cys and GA (blue ●), HbA1c (green Δ), and GapoA-I (red ×), respectively, for each individual monitored in panels a−c (Pearson's correlation, $n = 16$). (e) Correlation between the age of individual T2D patients and their levels of HSA-Cys (blue ●), HbA-SNO (green Δ), and apoA-I MetO (red ×), respectively (Pearson's correlation, $n = 8$).

increase of HSA-Cys in T2D compared to controls (mean = 49.59% vs 36.96%, $p = 0.0033$, Student's t test), a nonsignificant decrease of HbA-SNO (mean = 20.17% vs 19.33%, $p = 0.1489$, Student's t test), and a nonsignificant increase of apoA-I MetO (mean = 12.01% vs 12.87%, $p = 0.1212$, Student's t test). These results suggested the higher oxidative stress (via HSA-Cys) and

dx.doi.org/10.1021/pr401074t | J. Proteome Res. 2014, 13, 1560−1569

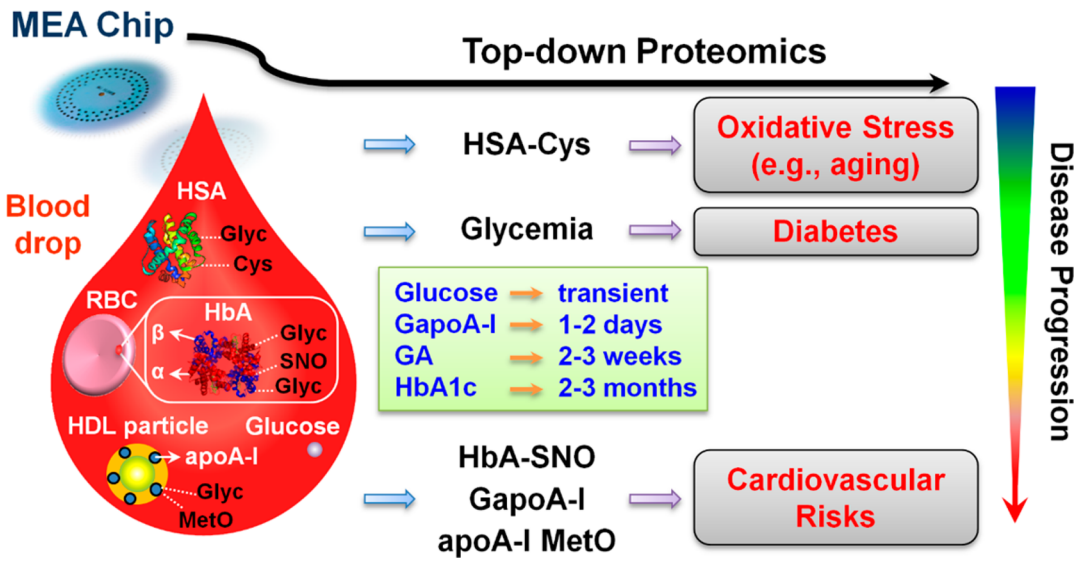

Figure 6. A scheme for rapid and multidimensional monitoring of diabetes using a drop of blood. Our top-down-proteomics-centric assay, enabled by our MEA chip platform, concurrently measures markers for multitime-scale glycemia (glucose, GapoA-I, GA, and HbA1c), oxidative stress (HSA-Cys), and cardiovascular risks (HbA-SNO, GapoA-I, and apoA-I MetO) in multiple compartments of blood, thereby contributing to better long-term monitoring and disease management of diabetes. The size of various components in the blood drop was not drawn to scale.

the possible perturbation of vasodilation functions (via GapoA-I and HbA-SNO) in T2D patients. Although we observed a significant increase of apoA-I glycation in T2D (Figure 4c), the nonsignificant change in the corresponding apoA-I MetO (Figure 5c) awaits further studies. We next evaluated whether oxidative stress interrelated with hyperglycemia in diabetes. We observed some nonsignificant correlations between HSA-Cys and blood glycemia markers HbA1c, GA, and GapoA-I, with the values for Pearson's correlation (two-tailed), $r = 0.4139$, $p = 0.1110$; $r = 0.4292$, $p = 0.0971$; and $r = 0.3110$, $p = 0.2410$ for GA, HbA1c, and GapoA-I, respectively (Figure 5d). We then investigated the possible cause of increased oxidative stress in T2D. We plotted the values of HSA-Cys, HbA-SNO, and apoA-I MetO against the ages available for the 8 T2D patients (Figure 5e). Interestingly, we observed a significant positive correlation between the age and HSA-Cys (Pearson's correlation, $r = 0.7087$, $p = 0.0491$, two-tailed), suggesting the increased oxidative stress during aging, which is consistent with the free-radical theory of aging. However, we did not observe a significant correlation between the age and HbA-SNO or between the age and apoA-I MetO. There have been conflicting results about the role and regulation of methionine oxidation of apoA-I in diabetes.[26,29,34,35] Future *in vitro* and *in vivo* studies will clarify the issue and provide new biological insights into the anti-atherosclerosis functions of HDL.[36,37]

■ DISCUSSION AND CONCLUSIONS

In this study, we have developed a novel assay for rapid and multidimensional monitoring of diabetes starting from a drop of blood (Figure 6). The key novelty of our assay lies in the combined analysis of small molecules, proteins, and protein post-translational modifications with common pathophysiological themes (high blood glucose and oxidative stress) that play important roles in diabetes, through a single LC−MS experiment using silicon-based microfluidic chips. We have considered several important issues during our assay development:

(A) Mass spectrometry response of different proteoforms. We assumed similar MS responses for unmodified and different adducts of HSA and apoA-I, respectively. This was mainly due to the fact that unlike HbA1c, highly purified and singly modified species of HSA and apoA-I were not available to us. We obtained a response factor of 0.9516 for HbA1c, which is very close to 1.0. Given that both apoA-I and HSA are bigger in size than HbA-β, one could presume that the effect of modifications (e.g., glycation) on MS would be bigger for HbA-β than for HSA and apoA-I. However, even if the response factor were not close to 1.0 for HSA and apoA-I, our assumption would not change our conclusions in a substantial way. First, we were interested in relative changes between normal and patient groups, using the percentage of each species. Second, our HSA and apoA-I results were consistent with those of HbA1c. Third, similar assumptions (i.e., response factor = 1.0) were made in earlier published works.[28,29] Finally, the main goal of this proof-of-principle work is to demonstrate one of the first top-down-proteomics-centric assays for clinical applications. Future work is certainly warranted to further validate our assumptions.

(B) Methionine oxidation (Met-ox). Met-ox is prominent in ESI analysis of peptides because Met residues are completely exposed to the reactive oxygen species (ROS) in the solution throughout the experiments. For proteins, Met-ox had been observed when the protein was acid-denatured prior to ESI analysis using high voltages.[38] In this case, HbA was acid-denatured first, which resulted in the complete exposure of Met residues in the β chain, for oxidation during ESI at 3.5 kV. Therefore, multiple Met-ox species were observed for HbA β chain. However, under our LC−MS conditions, we did not observe a significant population of Met-ox species for HbA β chain from the fresh whole blood, suggesting that the artificial contribution of Mex-ox during our ESI process was low. For the previous top-down MS analyses of apoA-I using the similar quantitation methods, samples had to go through a multistep sample preparation procedure including the immunoaffinity capture, wash, and elution prior to MS analysis.[26] In contrast, our one-step sample preparation included only a dilution step

dx.doi.org/10.1021/pr401074t | J. Proteome Res. 2014, 13, 1560−1569

for apoA-I in the plasma fraction and therefore would further minimize the artificial Met-ox formation during sample preparation. For apoA-I MetO calculation, we followed the concept of maximum methionine oxidation capacity by using the weighted oxidation of apoA-I in the numerator.[26] However, we included all identifiable apoA-I peaks in the denominator as the total apoA-I in order to be consistent with that in GapoA-I calculation.

(C) Absolute values of HbA1c and other glycemia by LC−MS measurements. Similar to calibrations for HbA1c values obtained from individual NGSP and IFCC platforms, each of the glycemia values determined by our assay might need calibrations in order to match those already adopted for clinical classification of nondiabetics and diabetics. For example, the current WHO cutoff value for HbA1c is 6.5%. A calibration factor could be applied to our data set to match this value.

Our method minimizes blood sample preparation prior to LC−MS analysis. Dynamic range is a challenging issue for both bottom-up proteomics and top-down proteomics. Our assay utilizes the three most abundant blood proteins for diabetes monitoring. It does not require complex sample preparation such as immunoaffinity enrichment and therefore is not constrained by the dynamic range issue that has long plagued other assays for analyzing low-abundance proteins. However, our MEA chip does contain an extraction segment that could be used for enrichment of additional low-abundance species for diabetes monitoring if needed. For conventional microbore/nanobore LC−MS systems, electrospray emitters are not monolithically coupled with LC columns but instead are connected via capillary tubing with proper fittings, which results in dead volumes and postcolumn losses. In addition, the micrometer-size nanospray emitters are easily clogged by plasma proteins because they are denatured under high ESI voltage and high organic solvents when eluted from the C4 column. This contributes to the low robustness and lack of reproducibility for nanospray MS and renders it unsuitable for clinical applications. Indeed, we observed significant clogging of capillary emitters (e.g., Picotip) interfaced to a commercial capillary C4 column during our initial method developments. In contrast, our microfabricated emitters are monolithically interfaced with the on-chip and online C4 column on the silicon-based MEA chip. This significantly reduces the clogging and minimizes the dead volume, thereby increasing the sensitivity and robustness while maintaining the specificity and accuracy of our nanoflow LC−MS assay. Our MEA chip has sustained the same level of performance after over 100 consecutive LC−MS runs of crude whole blood samples with essentially no sample cleanup. The 1-h LC−MS run was used in this work, but future optimization of the LC method and chip parameters, such as implementation of staggered parallel separation to increase the MS duty cycle,[39] could significantly shorten the total run time down to minutes for faster analysis, to be on par with the turnaround time of immunoassays. Implementation of multiplex and multifunction on-chip columns (e.g., 24-plex) on our MEA chip will further increase the throughput of our assay for parallel analysis of a large number of samples.

Our assay could provide new opportunities in understanding the biology and improving the long-term management of diabetes. Diabetes (including Type 1, Type 2, and Gestational) is a very complex and heterogeneous disease. The mechanisms underlying each subtypes of diabetes and how the oxidative stress induces both microvascular and cardiovascular complications of diabetes remain elusive.[32] Our assay directly monitors the oxidative stress using one key plasma marker, HSA-Cys, and possibly cardiovascular risks of diabetes using three potential markers including HbA-SNO, GapoA-I, and apoA-I MetO, concurrently with the corresponding status of longitudinal blood glycemia (glucose, HbA1c, GA, and GapoA-I). One of the major consequences of diabetes is cardiovascular diseases (CVD). In fact, heart attacks account for majority of the deaths in patients with diabetes. Both glycation and oxidation of apoA-I may affect the functions of HDL (a key player in CVD).[31,34,35,37] Therefore, our assay may facilitate longitudinal investigations of the initiation, progression, and consequences of diabetes for each individual and thus provide new insights at the molecular (proteins), cellular (RBCs), and tissue (blood) levels. This in turn might help dissect the mechanisms underlying diabetes and provide better disease management. The new FDA Guidance to Industry for the development of new anti-diabetes therapies mandates that their cardiovascular risks be evaluated concurrently for drug safety, in addition to demonstrating their efficacy of lowering and maintaining blood glucose levels. Our method simultaneously measures multiple biomarkers for blood glycemia, oxidative stress, and cardiovascular risks of individuals, using a single LC−MS run starting from a single drop of blood, and therefore may be used in conjunction with cardiac markers such as hERG (human potassium ion channel) in clinical trials to facilitate new drug developments. If further validated, our assay could be utilized for routine monitoring of patients, for example, in response to different treatment regimens, for personalized management and treatment of diabetes.

In summary, we have demonstrated a rapid, sensitive, and specific top-down-proteomics-centric clinical assay for monitoring multiclass biomarkers of diabetes starting from a drop of blood ($\leq$5 μL) using our MEA chip platform. If combined with the microsampling of blood (e.g., using calibrated capillary tubes) and validated with a larger patient population in conjunction with prospective clinical studies to determine the limit of detection (LOD), inter- and intrapatient variations, within- and between-day reproducibility, and comparability with the existing commercial platforms, our assay may contribute to the long-term management of diabetes and promote the clinical applications of top-down proteomics in theranostics of other diseases, for example, cancer and neurodegenerative diseases.

■ ASSOCIATED CONTENT

Supporting Information

This material is available free of charge via the Internet at http://pubs.acs.org.

■ AUTHOR INFORMATION

Corresponding Author

*Phone: 510-788-4069. Email: wang@newomics.com.

Author Contributions

D.W. conceived the study, designed and performed experiments, and wrote the manuscript. P.M. designed and performed experiments and wrote the manuscript.

Notes

The authors declare the following competing financial interest(s): Daojing Wang is the founder and Pan Mao is the

co-founder of Newomics Inc., which is commercializing some of the technologies described in this work.

■ ACKNOWLEDGMENTS

The authors acknowledge Grant Awards (R43ES022360 and R43ES023529) from the National Institute of Environmental Health Sciences and Contract Award HHSN261201300033C from the National Cancer Institute of the National Institutes of Health (to Newomics Inc.). The content is solely the responsibility of the authors and does not necessarily represent the official views of the National Institutes of Health. The authors thank Lawrence Berkeley National Laboratory and UC-Berkeley Marvell Nanofabrication Laboratory for facility access.

■ REFERENCES

(1) A.D.A.. Diagnosis and classification of diabetes mellitus. *Diabetes Care* **2013**, *36* (Suppl 1), S67−74.
(2) Little, R. R.; Rohlfing, C. L.; Sacks, D. B. Status of hemoglobin A1c measurement and goals for improvement: from chaos to order for improving diabetes care. *Clin. Chem.* **2011**, *57* (2), 205−14.
(3) Sacks, D. B. Measurement of hemoglobin A(1c): a new twist on the path to harmony. *Diabetes Care* **2012**, *35* (12), 2674−80.
(4) Cohen, R. M.; Holmes, Y. R.; Chenier, T. C.; Joiner, C. H. Discordance between HbA1c and fructosamine: evidence for a glycosylation gap and its relation to diabetic nephropathy. *Diabetes Care* **2003**, *26* (1), 163−7.
(5) Rodriguez-Segade, S.; Rodriguez, J.; Garcia Lopez, J. M.; Casanueva, F. F.; Camina, F. Estimation of the glycation gap in diabetic patients with stable glycemic control. *Diabetes Care* **2012**, *35* (12), 2447−50.
(6) Inaba, M.; Okuno, S.; Kumeda, Y.; Yamada, S.; Imanishi, Y.; Tabata, T.; Okamura, M.; Okada, S.; Yamakawa, T.; Ishimura, E.; Nishizawa, Y. Glycated albumin is a better glycemic indicator than glycated hemoglobin values in hemodialysis patients with diabetes: effect of anemia and erythropoietin injection. *J. Am. Soc. Nephrol.* **2007**, *18* (3), 896−903.
(7) Wang, D.; Bodovitz, S. Single cell analysis: the new frontier in 'omics'. *Trends Biotechnol.* **2010**, *28* (6), 281−90.
(8) Chen, R.; Mias, G. I.; Li-Pook-Than, J.; Jiang, L.; Lam, H. Y.; Miriami, E.; Karczewski, K. J.; Hariharan, M.; Dewey, F. E.; Cheng, Y.; Clark, M. J.; Im, H.; Habegger, L.; Balasubramanian, S.; O'Huallachain, M.; Dudley, J. T.; Hillenmeyer, S.; Haraksingh, R.; Sharon, D.; Euskirchen, G.; Lacroute, P.; Bettinger, K.; Boyle, A. P.; Kasowski, M.; Grubert, F.; Seki, S.; Garcia, M.; Whirl-Carrillo, M.; Gallardo, M.; Blasco, M. A.; Greenberg, P. L.; Snyder, P.; Klein, T. E.; Altman, R. B.; Butte, A. J.; Ashley, E. A.; Gerstein, M.; Nadeau, K. C.; Tang, H.; Snyder, M. Personal omics profiling reveals dynamic molecular and medical phenotypes. *Cell* **2012**, *148* (6), 1293−307.
(9) Boja, E.; Hiltke, T.; Rivers, R.; Kinsinger, C.; Rahbar, A.; Mesri, M.; Rodriguez, H. Evolution of clinical proteomics and its role in medicine. *J. Proteome Res.* **2010**, *10* (1), 66−84.
(10) Anderson, L.; Hunter, C. L. Quantitative mass spectrometric multiple reaction monitoring assays for major plasma proteins. *Mol. Cell. Proteomics* **2006**, *5* (4), 573−88.
(11) Whiteaker, J. R.; Zhao, L.; Anderson, L.; Paulovich, A. G. An automated and multiplexed method for high throughput peptide immunoaffinity enrichment and multiple reaction monitoring mass spectrometry-based quantification of protein biomarkers. *Mol. Cell. Proteomics* **2010**, *9* (1), 184−96.
(12) Van Eyk, J. E. Overview: the maturing of proteomics in cardiovascular research. *Circ. Res.* **2011**, *108* (4), 490−8.
(13) Smith, L. M.; Kelleher, N. L.; Linial, M.; Goodlett, D.; Langridge-Smith, P.; Ah Goo, Y.; Safford, G.; Bonilla, L.; Kruppa, G.; Zubarev, R.; Rontree, J.; Chamot-Rooke, J.; Garavelli, J.; Heck, A.; Loo, J.; Penque, D.; Hornshaw, M.; Hendrickson, C.; Pasa-Tolic, L.; Borchers, C.; Chan, D.; Young, N.; Agar, J.; Masselon, C.; Gross, M.; McLafferty, F.; Tsybin, Y.; Ge, Y.; Sanders, I.; Langridge, J.; Whitelegge, J.; Marshall, A. Proteoform: a single term describing protein complexity. *Nat. Methods* **2013**, *10* (3), 186−7.
(14) Tran, J. C.; Zamdborg, L.; Ahlf, D. R.; Lee, J. E.; Catherman, A. D.; Durbin, K. R.; Tipton, J. D.; Vellaichamy, A.; Kellie, J. F.; Li, M.; Wu, C.; Sweet, S. M.; Early, B. P.; Siuti, N.; LeDuc, R. D.; Compton, P. D.; Thomas, P. M.; Kelleher, N. L. Mapping intact protein isoforms in discovery mode using top-down proteomics. *Nature* **2011**, *480* (7376), 254−8.
(15) Liu, X.; Sirotkin, Y.; Shen, Y.; Anderson, G.; Tsai, Y. S.; Ting, Y. S.; Goodlett, D. R.; Smith, R. D.; Bafna, V.; Pevzner, P. A. Protein identification using top-down. *Mol. Cell. Proteomics* **2012**, *11* (6), M111 008524.
(16) Zinnel, N. F.; Pai, P. J.; Russell, D. H. Ion mobility-mass spectrometry (IM-MS) for top-down proteomics: increased dynamic range affords increased sequence coverage. *Anal. Chem.* **2012**, *84* (7), 3390−7.
(17) Ahlf, D. R.; Compton, P. D.; Tran, J. C.; Early, B. P.; Thomas, P. M.; Kelleher, N. L. Evaluation of the compact high-field orbitrap for top-down proteomics of human cells. *J. Proteome Res.* **2012**, *11* (8), 4308−14.
(18) Ansong, C.; Wu, S.; Meng, D.; Liu, X.; Brewer, H. M.; Deatherage Kaiser, B. L.; Nakayasu, E. S.; Cort, J. R.; Pevzner, P.; Smith, R. D.; Heffron, F.; Adkins, J. N.; Pasa-Tolic, L. Top-down proteomics reveals a unique protein S-thiolation switch in Salmonella Typhimurium in response to infection-like conditions. *Proc. Natl. Acad. Sci. U.S.A.* **2013**, *110* (25), 10153−8.
(19) Zhou, H.; Ning, Z.; Starr, A. E.; Abu-Farha, M.; Figeys, D. Advancements in top-down proteomics. *Anal. Chem.* **2012**, *84* (2), 720−34.
(20) Savaryn, J. P.; Catherman, A. D.; Thomas, P. M.; Abecassis, M. M.; Kelleher, N. L. The emergence of top-down proteomics in clinical research. *Genome Med.* **2013**, *5* (6), 53.
(21) Kim, W.; Guo, M.; Yang, P.; Wang, D. Microfabricated monolithic multinozzle emitters for nanoelectrospray mass spectrometry. *Anal. Chem.* **2007**, *79* (10), 3703−7.
(22) Mao, P.; Wang, H. T.; Yang, P.; Wang, D. Multinozzle emitter arrays for nanoelectrospray mass spectrometry. *Anal. Chem.* **2011**, *83* (15), 6082−9.
(23) Mao, P.; Gomez-Sjoberg, R.; Wang, D. Multinozzle emitter array chips for small-volume proteomics. *Anal. Chem.* **2013**, *85* (2), 816−9.
(24) Chen, C. J.; Chen, W. Y.; Tseng, M. C.; Chen, Y. R. Tunnel frit: a nonmetallic in-capillary frit for nanoflow ultra high-performance liquid chromatography-mass spectrometryapplications. *Anal. Chem.* **2012**, *84* (1), 297−303.
(25) Jeppsson, J. O.; Kobold, U.; Barr, J.; Finke, A.; Hoelzel, W.; Hoshino, T.; Miedema, K.; Mosca, A.; Mauri, P.; Paroni, R.; Thienpont, L.; Umemoto, M.; Weykamp, C. Approved IFCC reference method for the measurement of HbA1c in human blood. *Clin. Chem. Lab. Med.* **2002**, *40* (1), 78−89.
(26) Yassine, H.; Borges, C. R.; Schaab, M. R.; Billheimer, D.; Stump, C.; Reaven, P.; Lau, S. S.; Nelson, R. Mass spectrometric immunoassay and MRM as targeted MS-based quantitative approaches in biomarker development: potential applications to cardiovascular disease and diabetes. *Proteomics Clin. Appl.* **2013**, *7* (7−8), 528−40.
(27) Funk, W. E.; Li, H.; Iavarone, A. T.; Williams, E. R.; Riby, J.; Rappaport, S. M. Enrichment of cysteinyl adducts of human serum albumin. *Anal. Biochem.* **2010**, *400* (1), 61−8.
(28) Boisvert, M. R.; Koski, K. G.; Skinner, C. D. Increased oxidative modifications of amniotic fluid albumin in pregnancies associated with gestational diabetes mellitus. *Anal. Chem.* **2010**, *82* (3), 1133−7.
(29) Borges, C. R.; Oran, P. E.; Buddi, S.; Jarvis, J. W.; Schaab, M. R.; Rehder, D. S.; Rogers, S. P.; Taylor, T.; Nelson, R. W. Building multidimensional biomarker views of type 2 diabetes on the basis of protein microheterogeneity. *Clin. Chem.* **2011**, *57* (5), 719−28.
(30) Anraku, M.; Chuang, V. T.; Maruyama, T.; Otagiri, M. Redox properties of serum albumin. *Biochim. Biophys. Acta* **2013**, *1830* (12), 5465−72.

(31) Brown, B. E.; Nobecourt, E.; Zeng, J.; Jenkins, A. J.; Rye, K. A.; Davies, M. J. Apolipoprotein A-I glycation by glucose and reactive aldehydes alters phospholipid affinity but not cholesterol export from lipid-laden macrophages. *PLoS One* **2013**, *8* (5), e65430.
(32) Giacco, F.; Brownlee, M. Oxidative stress and diabetic complications. *Circ. Res.* **2010**, *107* (9), 1058−70.
(33) Lima, B.; Forrester, M. T.; Hess, D. T.; Stamler, J. S. S-nitrosylation in cardiovascular signaling. *Circ. Res.* **2010**, *106* (4), 633−46.
(34) Panzenbock, U.; Kritharides, L.; Raftery, M.; Rye, K. A.; Stocker, R. Oxidation of methionine residues to methionine sulfoxides does not decrease potential antiatherogenic properties of apolipoprotein A-I. *J. Biol. Chem.* **2000**, *275* (26), 19536−44.
(35) Shao, B.; Cavigiolio, G.; Brot, N.; Oda, M. N.; Heinecke, J. W. Methionine oxidation impairs reverse cholesterol transport by apolipoprotein A-I. *Proc. Natl. Acad. Sci. U.S.A.* **2008**, *105* (34), 12224−9.
(36) Jaouad, L.; de Guise, C.; Berrougui, H.; Cloutier, M.; Isabelle, M.; Fulop, T.; Payette, H.; Khalil, A. Age-related decrease in high-density lipoproteins antioxidant activity is due to an alteration in the PON1's free sulfhydryl groups. *Atherosclerosis* **2006**, *185* (1), 191−200.
(37) Navab, M.; Reddy, S. T.; Van Lenten, B. J.; Fogelman, A. M. HDL and cardiovascular disease: atherogenic and atheroprotective mechanisms. *Nat. Rev. Cardiol.* **2011**, *8* (4), 222−32.
(38) Boys, B. L.; Kuprowski, M. C.; Noel, J. J.; Konermann, L. Protein oxidative modifications during electrospray ionization: solution phase electrochemistry or corona discharge-induced radical attack? *Anal. Chem.* **2009**, *81* (10), 4027−34.
(39) Livesay, E. A.; Tang, K.; Taylor, B. K.; Buschbach, M. A.; Hopkins, D. F.; LaMarche, B. L.; Zhao, R.; Shen, Y.; Orton, D. J.; Moore, R. J.; Kelly, R. T.; Udseth, H. R.; Smith, R. D. Fully automated four-column capillary LC−MS system for maximizing throughput in proteomic analyses. *Anal. Chem.* **2008**, *80* (1), 294−302.